Journal of Thermal Analysis and Calorimetry
https://doi.org/10.1007/s10973-026-15476-6

Examination of multiple approaches to kinetic modelling of biomass pyrolysis: case study on spruce wood powder pyrolysis in nitrogen atmosphere under non-isothermal conditions

Jure Voglar[1] · **Blaž Likozar**[1,2,3,4]

Received: 19 May 2025 / Accepted: 16 March 2026

Abstract
Several approaches to kinetic modelling of biomass pyrolysis were examined and critically evaluated based on a case study of spruce wood powder pyrolysis in nitrogen atmosphere under non-isothermal conditions with different heating rates and carrier gas flow rates. The pyrolysis modelling approaches analyzed: modelling with multiple Gaussians, isoconversional kinetic models by Fridman (FR), Ozawa-Flynn-Wall (OFW), and Kissinger–Akahira–Sunose (KAS), as well as an integrated kinetics-transport pyrolysis model. The multiple Gaussian model exhibited high quality of fits, with an average coefficient of determination of 0.9933. It was found to be easy to implement, allowed determination of major pseudo-components, and its parameters could be used to estimate kinetic parameters. Isoconversional approaches have a limited range of validity, especially in biomass pyrolysis, and are therefore not recommended for use with biomass pyrolysis thermogravimetric data sets. The newly adapted integrated kinetics-transport pyrolysis model exhibited sufficient quality of fits to the data across a wide range of experimental conditions, indicating robustness and universal applicability to biomass pyrolysis. It also has the potential to be modified to describe the pyrolysis of other materials. The average coefficient of determination, evaluated based on the conversion rate of the integrated kinetics-transport pyrolysis model, was 0.9348. The integrated kinetics-transport pyrolysis model describes both physical and chemical phenomena during the pyrolysis process.

Keywords Spruce wood · Non-isothermal pyrolysis · Modelling · Kinetics · Statistical analysis

Introduction

Pyrolysis of biomass is a thermochemical conversion process involving a complex set of concurrent and competitive reactions under oxygen-depleted conditions [1]. Biomass includes organic materials derived from plants and animals, and is considered a vast, renewable resource with significant energy potential. Biomass is classified by origin into woody, herbaceous, and animal-derived categories [2].

Kinetic models of biomass pyrolysis are divided into two categories: (i) lumped and (ii) distributed models, depending on the reaction mechanism of the pyrolysis process. Lumped models group individual species into three product classes: gas, tar and char, with their kinetic schemes for primary and secondary degradation. Some also consider the three main components of biomass: hemicellulose, cellulose, and lignin, and their thermal decomposition. Distributed (activation energy) models assume that pyrolysis products are formed by an infinite number of independent parallel reactions with different activation energies distributed according to a Gaussian function [3]. Other pyrolysis process models include heat and mass transport models, particle models, reactor models, and artificial neural network (ANN) models [1].

Recently, biomass pyrolysis has also been modelled with multiple Gaussians, each one representing one pseudo-component. This modelling approach is especially useful to

✉ Jure Voglar
jure.voglar@ki.si

[1] Department of Catalysis and Chemical Reaction Engineering, National Institute of Chemistry, Hajdrihova 19, 1001 Ljubljana, Slovenia

[2] Faculty of Chemistry and Chemical Technology, University of Ljubljana, Večna Pot 113, 1001 Ljubljana, Slovenia

[3] Faculty of Chemistry and Chemical Engineering, University of Maribor, Smetanova Ulica 17, 2000 Maribor, Slovenia

[4] Faculty of Polymer Technology, Ozare 19, 2380 Slovenj Gradec, Slovenia

Published online: 13 April 2026

identify the major components of biomass during pyrolysis. The model describes the behavior of the conversion rate in the temperature domain well [4, 5]. This method has been applied to tobacco straw pyrolysis [4] and pyrolysis of macadamia nut peel [5]. However, the parameters obtained from the multiple Gaussians have not yet correlated with kinetic parameters such as activation energies.

Isoconversional kinetic models have been used to describe the pyrolysis of various biomass resources, such as wood [6], corn stalk [7], agricultural biomass wastes [8], soybean stalk [9], cattle manure [10], and flax shives [11]. However, as these models were originally developed for studying polymer decomposition and later extended to biomass pyrolysis [12], they have substantial drawbacks when modelling biomass pyrolysis. For example, isoconversional models have been found to poorly describe pyrolysis phenomena at low (below 0.2) and high (above 0.8) levels of conversion [13]. Therefore, they should be used with care and primarily during the initial stages of pyrolysis data analysis, especially when complex materials such as biomass are considered [14].

Our previous work [15] presented an integrated kinetics-transport pyrolysis model, in which pyrolysis kinetics considering four pseudo-components with first-order thermal decomposition reactions, internal heat transfer (within the sample), and external mass transport were modelled. The model accurately described the thermal degradation of dry hemp (*Cannabis sativa* L.) biomass under various conditions: heating rate, carrier gas flow rate, particle size, and plant part (roots, stems, and leaves). The non-isothermal pyrolysis experiments were conducted in nitrogen atmosphere under 12 different conditions, and the model was robust enough to fit the experimental conversion degree values, with an average coefficient of determination of 0.9980. Since the thermogravimetric instrument was changed, the existing model was modified accordingly and tested during pyrolysis of spruce wood powder in nitrogen atmosphere. The kinetic part of the model remains unchanged and considers the thermal degradation of four main pseudo-components: volatiles, hemicellulose, cellulose, and lignin, all with first-order of reactions. The modified integrated kinetics-transport pyrolysis model is not the only one that accounts for both kinetics and transport phenomena during pyrolysis. Babu and Chaurasia [16] developed three different kinetic-transport pyrolysis models, validated and compared them using data from pyrolysis of cylindrical wood samples. Numerical approaches to modelling kinetics and transport phenomena during pyrolysis usually focus on a single particle and are based on computational fluid dynamics (CFD) [17] or other finite element modelling software [18].

The aim of this paper is to assess the strengths and weaknesses of different modelling approaches commonly used to process data from thermogravimetric analyses. The examined models include (i) the multicomponent Gaussian model, (ii) isoconversional kinetic models by Fridman (FR), Ozawa-Flynn-Wall (OFW), and Kissinger–Akahira–Sunose (KAS), and (iii) an integrated kinetics-transport pyrolysis model. This work provides pyrolysis experts with valuable new knowledge about kinetic modelling of biomass pyrolysis.

Materials and methods

Spruce wood biomass sample

The spruce wood powder sample was prepared in order to obtain small particles allowing to limit the effect of temperature lags. This was done by using a rasp on a piece of dried, unpainted spruce wood held in place by a workshop bench vice and collecting the powder that fell from the rasp-sample interface. The spruce wood powder sample contained particles smaller than 1 mm. More details on the preparation protocol and the maximum particle size estimation are available in Online Resource 1 (ESM_1).

Thermogravimetry

Pyrolysis of the spruce wood powder sample was investigated using thermogravimetry (TG) with the Q5000 IR instrument (TA Instruments, New Castle, Delaware, USA). Experiments were conducted in nitrogen (N_2) atmosphere under non-isothermal conditions at heating rates (β) of 5, 10, 15, 20, and 25 K min^{-1}, with N_2 flow rate (Q) 50 mL min^{-1}, and at N_2 volumetric flow rates of 10, 20, 30, 40, and 50 mL min^{-1}, with a heating rate of 5 K min^{-1}. Various heating rates and N_2 flow rates were tested to assess the robustness of the kinetic models. The initial mass of the samples placed in the TG instrument ranged from 12.2 to 19.0 mg, with an average of 16.4 mg. The relatively high initial masses (above 10.0 mg) were chosen to maintain precise mass measurements by minimizing relative measurement errors. The authors note that measurement # 1, with the lowest heating rate and highest carrier gas flow rate in the experimental matrix, should closely reflect the true kinetic behavior of the material's thermal decomposition, as a low heating rate minimizes temperature gradients within the material and between the material and the temperature sensor, while a high carrier gas flow rate ensures rapid removal of gaseous products from the specimen, so kinetic limitations dominate under these conditions. In all other measurement conditions (except # 1), the models must compensate for heat and mass transport limitations to achieve accuracy. Measurements were always performed in the temperature range from 30 to 800 °C. The TG experimental matrix is presented in Table 1.

Table 1 TG experimental matrix

#	β/K min^{-1}	Q/mL min^{-1}
1	5	50
2	10	50
3	15	50
4	20	50
5	25	50
6	5	10
7	5	20
8	5	30
9	5	40

Modelling of pyrolysis

The pyrolysis kinetic model fitting was carried out in the Python programming language using the Spyder integrated development environment (IDE).

Modelling of pyrolysis with Gaussians

The conversion (X_i) of pseudo-component (i) during pyrolysis is defined by Eq. 1, where $m_{i,s}$ is the initial mass, $m_{i,f}$ is the final mass, and m_i is the current mass. In the literature dealing with pyrolysis, the conversion degree (X in this work) is usually denoted with small Greek letter alpha (α).

$$X_i = \frac{m_{i,s} - m_i}{m_{i,s} - m_{i,f}} \tag{1}$$

The conversion rate of the biomass (dX/dt) is modelled with Eq. 2, where w_i is the mass fraction of pseudo-component (i), and a_i, b_i and c_i are parameters of the Gaussian for pseudo-component i, T is the temperature of the biomass (in Kelvin), and n is the total number of pseudo-components. In this work, the pseudo-components of the multiple Gaussians model are denoted as follows: volatiles ($i=1$), hemicellulose ($i=2$), cellulose ($i=3$), and lignin ($i=4$). The parameter a_i is proportional to the height of the curve's peak, b_i indicates the position of the center of the peak, and c_i (standard deviation) controls the width of the "bell".

$$\frac{dX}{dt} = \sum_{i=1}^{n} w_i \frac{dX_i}{dt} = \sum_{i=1}^{n} a_i e^{-\left(\frac{(T-b_i)^2}{2 \cdot c_i^2}\right)} \tag{2}$$

Isoconversional kinetic models

Three different isoconversional kinetic models found in [7] were tested. The first is the Fridman (FR) model, described by Eq. 3, where β is the heating rate of the sample, A_X is the pre-exponential factor at conversion X, $f(X)$ is the differential form of the conversion function ($f(X) = 1 - X$), $E_{a,X}$ is the activation energy at conversion X, and R is the universal gas constant (8.314 J mol^{-1} K^{-1}).

$$\ln\left[\beta\left(\frac{dX}{dT}\right)\right] = \ln\left[A_X f(X)\right] - \frac{E_{a,X}}{RT} \tag{3}$$

The Ozawa-Flynn-Wall (OFW) model is defined by Eq. 4, where $g(X)$ is the integral form of the conversion function ($g(X) = -\ln(1-X)$).

$$\ln[\beta] = \ln\left[\frac{A_X E_{a,X}}{R g(X)}\right] - 5.331 - 1.052\frac{E_{a,X}}{RT} \tag{4}$$

The third tested model (Eq. 5) is the Kissinger–Akahira–Sunose (KAS) model.

$$\ln\left[\beta/T^2\right] = \ln\left[\frac{RA_X}{E_{a,X} g(X)}\right] - \frac{E_{a,X}}{RT} \tag{5}$$

All of the above isoconversional kinetic models require data from at least two different heating rates to determine the kinetic parameters. At the specified degree(s) of conversion (X), the line(s) should accurately describe the models in the domain of the reciprocal temperature of the sample ($1/T$). The slope of the line defines the activation energy at the specified conversion. A detailed description of the processing of thermogravimetric analysis data for isoconversional kinetic analysis of lignocellulosic biomass pyrolysis is available in [7].

Integrated kinetics-transport pyrolysis model

Since a different thermogravimetric measuring device was used in our previous experiments [15], where the temperature sensor is in contact with the outer surface of the sample, the heat transfer model was modified to account for the heat transfer resistance between the center of the sample and the temperature sensor. In the current case, the temperature is measured laterally to the sample (in the flow of the carrier gas). The modification to the heat transfer model enhanced the universality, flexibility, and applicability of the integrated pyrolysis model. The newly developed model still uses four pseudo-components to kinetically describe biomass pyrolysis. Four pseudo-components (i) were considered in the kinetic modelling: volatiles ($i=1$), hemicellulose ($i=2$), cellulose ($i=3$), and lignin ($i=4$). Transport was modelled in terms of external mass transfer between the sample and the carrier gas, and heat transfer between the center of the sample and the temperature sensor.

The sample's overall conversion (X) is the sum of the individual pseudo-component conversions X_i multiplied by their mass fractions w_i (Eq. 6).

$$X = \sum_{i=1}^{n} w_i X_i \tag{6}$$

Kinetics was modelled with a first-order differential equation (Eq. 7), where external mass transport limitations were neglected (at the highest carrier gas flow rate of 50 mL min^{-1}).

$$\frac{dX_i}{dt} = A_i e^{\left(-\frac{E_{a,i}}{RT}\right)}\left(1 - X_i\right) \tag{7}$$

In cases with significant external mass transport resistance (at N_2 flow rates below 50 mL min^{-1}), kinetics and mass transport were modelled using two first-order differential equations (Eqs. 8 and 9). Here $X_{a,i}$ represents the kinetics limited pseudo-component's conversion, X_i represents the kinetics and mass transport limited pseudo-component's conversion, k_l is the external mass transport coefficient, and a is the ratio of surface area to volume of the pyrolyzed material. The initial guess for $k_l a$ was estimated to be $1.0 \cdot 10^{-2}$ s^{-1}, based on our previous work [15], and was allowed to vary during execution of the algorithm.

$$\frac{dX_i}{dt} = k_l a\left(X_{a,i} - X_i\right) \tag{8}$$

$$\frac{dX_{a,i}}{dt} = A_i e^{\left(-\frac{E_{a,i}}{RT}\right)}\left(1 - X_{a,i}\right) \tag{9}$$

The measured temperature T_m (at the temperature sensor) was described by the first-order differential equation (Eq. 10).

$$\frac{dT_m}{dt} = \beta \tag{10}$$

The heat transfer between the sensor and the center of the sample was modelled with the first-order differential equation (Eq. 11), where ρ is the density of the sample, V is the volume of the sample, C_p is the specific heat of the sample, R_t is the thermal resistance between the center of the sample and the temperature sensor and γ is the heat transfer constant. The initial guess for γ ($7.2 \cdot 10^{-2}$ s^{-1}) was calculated based on an assessment of the sample´s geometry, its material properties, and the thermal resistance, which includes both convection and conduction. The γ parameter was then adjusted by the optimization algorithm.

$$\frac{dT}{dt} = \frac{1}{\rho V C_p R_t}\left(T_m - T\right) = \gamma\left(T_m - T\right) \tag{11}$$

Therefore, kinetics and heat transfer modelling involve solving a system of three first-order differential equations (Eqs. 7, 10, and 11), while modelling kinetics, heat transfer, and external mass transport requires solving a system of four first-order differential equations (Eqs. 8–11).

Results and discussion

The measured TG dataset is available in Online Resource 2 (ESM_2).

Description of pyrolysis with Gaussians

The sum of four Gaussian functions describes the measured TG data well, with coefficients of determination (R^2) ranging from 0.9931 to 0.9935 and an average value of 0.9933. This method is one of the easiest to implement, especially as an initial step in the analysis of TG data, and helps identify the number of major pseudo-components in the sample. However, the obtained Gaussian parameters, available in Online Resource 3 (ESM_3), at this stage appear to provide little useful information about the pyrolysis process itself.

A graphical representation of the fitted multiple Gaussian model is shown in Fig. 1. Despite the model's relative simplicity and the ease and high speed of the fitting procedure, it accurately captures the observed conversion rate in the temperature domain. Plots of all Gaussian fits are available in Online Resource 4 (ESM_4).

Testing of isoconversional kinetic models

The TG data was also analyzed using isoconversional kinetic models by Fridman (FR), Ozawa-Flynn-Wall (OFW), and Kissinger–Akahira–Sunose (KAS), as described in "Isoconversional kinetic models" section. The results are presented in both numerical (Table 2) and graphical (Fig. 2) formats, with additional graphs available in Online Resource 5 (ESM_5). There are few differences in the activation energies calculated by the three models; in particular the OFW and KAS models yield almost identical results.

The coefficient of determination exceeds 0.90 for most conversion values, but this is not the case at high conversion degrees. R^2 begins to fall rapidly above a conversion degree of 0.850 and starts to rise again 0.925. These abrupt changes are associated with rapid fluctuations in the calculated activation energies. At conversions above 0.825, the activation energy values tend to increase rapidly, followed by a sharp drop to negative values at conversions above 0.900. Considering all observed properties of the selected isoconversional kinetic models, researchers are strongly advised to use other models to accurately describe biomass pyrolysis

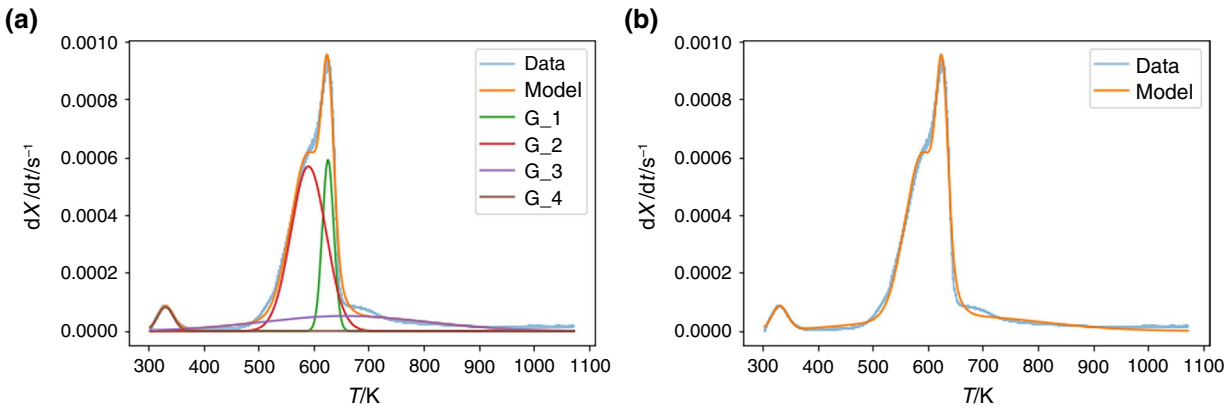

Fig. 1 Example of Gaussian fit for conversion rate in the temperature domain of data # 1 **a** with individual Gaussians representing pseudo-components and **b** the overall model only

or to use the presented isoconversional kinetic models only at the initial stages of TG data analysis and/or for validation of other kinetic models.

A similar trend as shown in Fig. 2a was also observed by Cai et al. [7] in their case study on the pyrolysis of corn stalk, where activation energy rises, plateaus, and rises again with increasing conversion. They did not display results beyond a conversion of 0.85 and did not offer any specific explanation for this. At a conversion of 0.85, they reported a significantly lower coefficient of determination (R^2), below 0.90 (0.8998), compared to lower conversions.

Application of integrated kinetics-transport pyrolysis model

Our modified kinetics-transport pyrolysis model was applied to all measured TG data for spruce wood powder pyrolysis. The modelling results are shown in Fig. 3. The model fits the data relatively well, except in the temperature region between 400 and 600 °C. The fits could potentially be improved if (i) another pseudo-component was added, as done by Cano-Pleite et al. [19], but this would not reflect the actual sample composition, or (ii) a higher reaction order for lignin decomposition were used, which could be implemented quite easily. However, Jiang et al. [20] reported that the pyrolysis of all lignins except Klason lignin (which has an order of 1.5) is first order with respect to solid decomposition. Therefore, the model was kept unchanged to align with the current understanding of spruce wood biomass chemical composition and pyrolysis behavior.

The TG data presented in Fig. 3 shows the effects of heating rate (β) variation (Fig. 3a, b) and carrier gas (N_2) flow rate (Q) variation (Fig. 3c, d), as observed experimentally by multiple researchers. Both the relative mass and mass loss rate curves shift to a higher temperature range with increasing heating rate, a phenomenon known as thermal hysteresis [4]. The main cause of the delayed thermal degradation process at high heating rates is the significant temperature difference between the surface and interior of the particles, making conduction heat transfer resistance an important factor [21]. The thermal hysteresis phenomenon has been observed by several researches, including Jiang et al. [22]. Regarding the effects of carrier gas flow rate variation, the data points almost completely overlap. Therefore, there is a negligible effect of nitrogen gas flow rate variations in the range from 10 to 50 mL min^{-1} in experiments # 6–9 and # 1 using the Q5000 IR instrument. Similar negligible effects of nitrogen flow rate were reported in laboratory scale TG experiments on tire rubber pyrolysis [23]. The small influence of carrier gas flow rate variations in laboratory scale pyrolysis experiments may be reason most researchers focus only on changing the heating rate, e.g., [24, 25]. Table 3 presents values related to the composition of spruce wood biomass and its pyrolysis kinetic parameters. As spruce is a major softwood species, the typical composition of softwoods was referenced from the literature. Softwood species typically contain 33–42% cellulose, 22–40% hemicellulose, 27–32% lignin, and 2–3.5% extractives [26]. The calculated mass fraction of volatiles, 4.1%, is slightly higher than the upper limit for extractives (3.5%), which could be explained by additional moisture in the wood sample. The hemicellulose fraction of 30.7% falls within the typical range (22–40%) for softwoods. However, the calculated values of mass fractions of cellulose (20.2%) and lignin (45.0%) are outside the typical softwood concentrations. The cellulose content is underestimated, as its typical lower limit is 33%, and the lignin content is significantly overestimated, with its typical upper limit at 32%. The calculated mass fractions of the three main components: hemicellulose, cellulose, and lignin are in some cases outside the typical limits for softwoods. However,

Table 2 Results of testing the three isoconversional kinetic models (FR, OFW, and KAS) on data # 1 to # 5 with their corresponding coefficients of determination

X	$E_{a,FR}$/kJ mol^{-1}	$E_{a,OFW}$/kJ mol^{-1}	$E_{a,KAS}$/kJ mol^{-1}	R^2_{FR}	R^2_{OFW}	R^2_{KAS}
0.025	36.6	64.1	61.6	0.9337	0.9725	0.9672
0.050	162.0	98.8	95.6	0.9740	0.9895	0.9877
0.075	197.5	174.2	174.4	0.9977	0.9927	0.9920
0.100	204.2	194.1	195.2	0.9950	0.9966	0.9964
0.125	199.2	198.2	199.3	0.9952	0.9959	0.9955
0.150	195.9	196.8	197.7	0.9923	0.9940	0.9935
0.175	193.0	196.5	197.3	0.9919	0.9937	0.9931
0.200	196.8	195.5	196.2	0.9941	0.9950	0.9946
0.225	193.6	193.2	193.6	0.9936	0.9949	0.9944
0.250	193.8	193.7	194.1	0.9959	0.9946	0.9940
0.275	193.3	192.4	192.6	0.9937	0.9943	0.9938
0.300	193.1	193.7	193.9	0.9946	0.9951	0.9946
0.325	191.2	194.0	194.2	0.9920	0.9940	0.9934
0.350	195.6	193.5	193.6	0.9938	0.9941	0.9935
0.375	192.2	194.1	194.2	0.9945	0.9954	0.9950
0.400	190.2	192.1	192.0	0.9939	0.9951	0.9946
0.425	192.8	192.9	192.8	0.9931	0.9941	0.9935
0.450	192.4	194.5	194.5	0.9958	0.9954	0.9950
0.475	194.3	193.3	193.1	0.9943	0.9948	0.9943
0.500	191.3	191.6	191.2	0.9952	0.9954	0.9949
0.525	191.2	192.0	191.6	0.9960	0.9952	0.9947
0.550	189.7	191.3	190.8	0.9966	0.9959	0.9954
0.575	186.0	189.2	188.6	0.9967	0.9972	0.9969
0.600	185.3	188.9	188.3	0.9961	0.9950	0.9945
0.625	183.8	188.2	187.5	0.9961	0.9973	0.9971
0.650	184.9	191.5	190.8	0.9965	0.9964	0.9961
0.675	188.3	191.1	190.4	0.9974	0.9964	0.9961
0.700	188.3	189.0	188.2	0.9968	0.9964	0.9960
0.725	190.8	189.0	188.2	0.9967	0.9970	0.9967
0.750	194.9	187.8	186.9	0.9970	0.9964	0.9961
0.775	202.1	190.3	189.4	0.9965	0.9965	0.9962
0.800	219.1	194.6	193.9	0.9957	0.9958	0.9953
0.825	261.0	202.0	201.6	0.9916	0.9956	0.9952
0.850	452.4	259.3	261.8	0.9523	0.9858	0.9846
0.875	553.8	479.9	493.6	0.7798	0.8025	0.7952
0.900	651.8	582.9	601.5	0.6953	0.6937	0.6854
0.925	−215.5	−114.9	−133.2	0.0378	0.0174	0.0210
0.950	−336.6	−271.4	−298.9	0.6356	0.5826	0.6047
0.975	−242.4	−175.6	−199.8	0.8058	0.7457	0.7743

these are pseudo-components and not the actual composition of the spruce wood sample, and all main components have mass fractions above 20%, indicating that none was greatly underestimated.

Examining the activation energies, the value for volatiles (71.9 kJ mol^{-1}) is slightly higher than that observed by Voglar et al. [15], which was 62.8 kJ mol^{-1}. The activation energy of hemicellulose, 102.5 kJ mol^{-1}, is comparable to the value (95.4 kJ mol^{-1}) reported by Yeo et al. [27]. The activation energy for cellulose, 133.3 kJ mol^{-1}, agrees well with the value of 133.0 kJ mol^{-1} calculated by Hajaligol et al. [28]. Lignin's activation energy (167.5 kJ mol^{-1}) matches the observation of Mani et al. [29], where the distribution of the activation energy of lignin pyrolysis peaks in the range of 158–170 kJ mol^{-1}.

The pre-exponential factors span a wide range of values across multiple orders of magnitude, consistent with observations in the biomass pyrolysis literature, where large

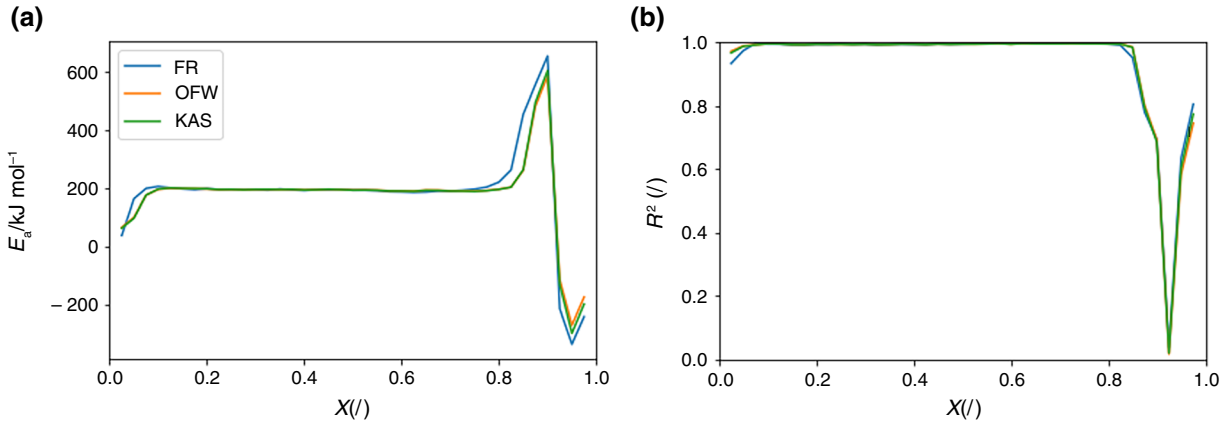

Fig. 2 Calculated **a** activation energy in the domain of conversion and **b** coefficient of determination (R^2) in the domain of conversion for the three isoconversional kinetic models (FR, OFW, and KAS) for data # 1 to # 5

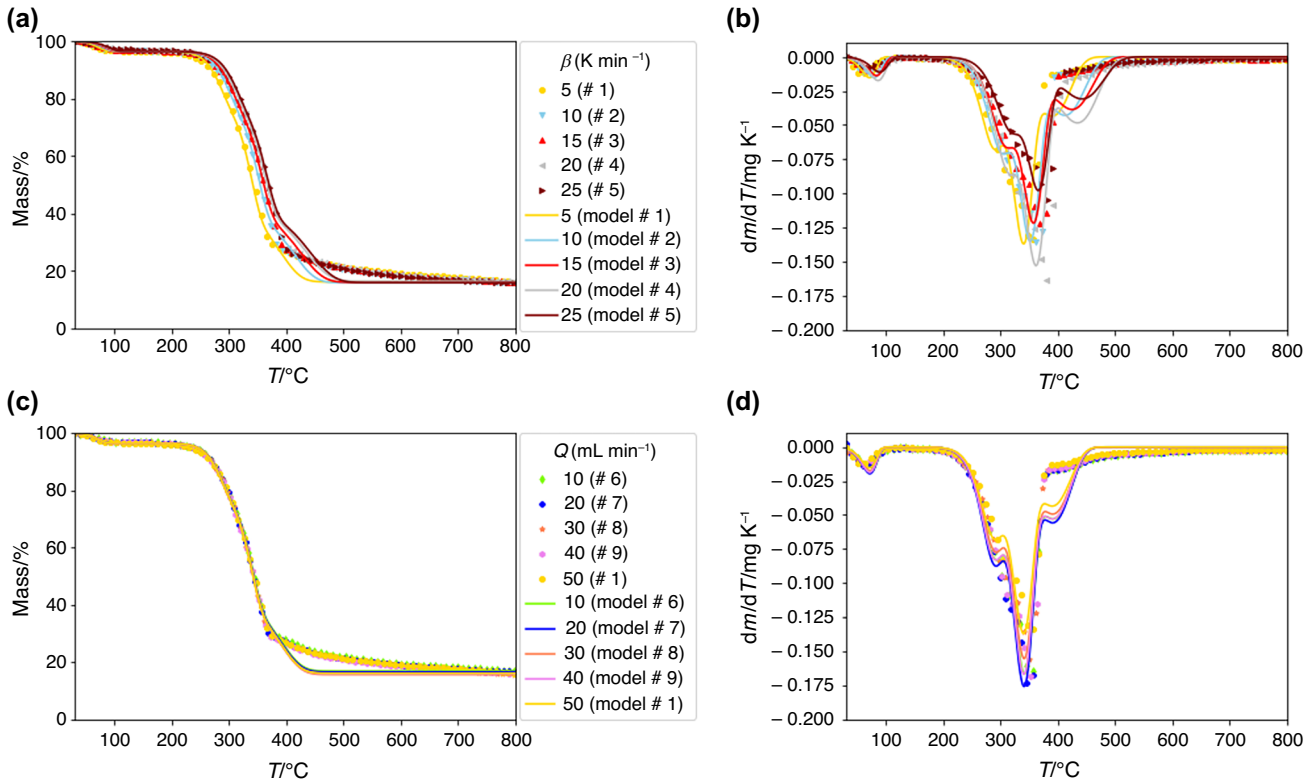

Fig. 3 Relative mass and mass loss rate in the temperature domain at different heating rates (**a**, **b**) and carrier gas flow rates (**c**, **d**) using the integrated kinetics-transport pyrolysis model for the data

discrepancies in A values are found for different biomass materials [30] as well as for a single material [31].

Table 4 shows that the integrated kinetics-transport pyrolysis model provides a satisfactory fit to the TG data, with coefficients of determination ranging from 0.9930 to 0.9964 and an average value of 0.9950. The heat transfer constant (γ) increases monotonically from data # 1 to # 5, most likely due to altered thermal properties (e.g., thermal conductivity) of the sample as a consequence of changing heating rate (thermal degradation rate). The heat transfer constant was assumed to be a function only of the heating rate and was therefore the same for data # 1 and # 6–9. The parameters describing external mass transport (k_la) generally show an increasing trend from data # 6 to # 9, as expected, since increasing the carrier gas flow rate enhances the convective transport of species from the sample. However, there

Table 3 Spruce wood biomass pseudo-component (i) composition with kinetic parameters for four pseudo-components (i) during pyrolysis in nitrogen atmosphere (volatiles ($i=1$), hemicellulose ($i=2$), cellulose ($i=3$), lignin ($i=4$))

w_1	0.041
w_2	0.307
w_3	0.202
w_4	0.450
$E_{a,1}$/kJ mol^{-1}	71.9
$E_{a,2}$/kJ mol^{-1}	102.5
$E_{a,3}$/kJ mol^{-1}	133.3
$E_{a,4}$/kJ mol^{-1}	167.5
A_1/s^{-1}	$6.41 \cdot 10^{8}$
A_2/s^{-1}	$3.05 \cdot 10^{5}$
A_3/s^{-1}	$1.64 \cdot 10^{10}$
A_4/s^{-1}	$1.07 \cdot 10^{12}$

Table 4 Calculated heat transfer coefficients (γ), external mass transport coefficients ($k_l a$) and coefficients of determination (R^2)

#	γ/s^{-1}	$k_l a$/s^{-1}	R^2
1	$2.30 \cdot 10^{-2}$	/	0.9930
2	$5.38 \cdot 10^{-2}$	/	0.9960
3	$1.98 \cdot 10^{-1}$	/	0.9959
4	$6.11 \cdot 10^{-1}$	/	0.9964
5	$1.38 \cdot 10^{0}$	/	0.9962
6	$2.30 \cdot 10^{-2}$	$6.27 \cdot 10^{-2}$	0.9943
7	$2.30 \cdot 10^{-2}$	$1.43 \cdot 10^{-1}$	0.9949
8	$2.30 \cdot 10^{-2}$	$8.26 \cdot 10^{-2}$	0.9934
9	$2.30 \cdot 10^{-2}$	$2.87 \cdot 10^{-1}$	0.9945

is a deviation from this overall increasing trend at data # 7, which can be explained by the actual dependency of the heat transfer constant on the carrier gas flow rate, a factor not explicitly accounted for.

Statistical evaluation of the kinetic models

All tested models were previously evaluated using the coefficient of determination (R^2). However, the R^2 value (between models and data) was initially calculated for different quantities. The model with multiple Gaussians was evaluated for the goodness of fit of the conversion rate (dX/dt), while isoconversional kinetic models were evaluated for linear fits of $\ln[\beta(dX/dT)]$, $\ln[\beta]$, and $\ln[\beta/T^2]$ for the FR, OFW, and KAS models, respectively. The integrated kinetics-transport pyrolysis model was evaluated in terms of conversion (X). Therefore, direct comparison of R^2 values calculated for different quantities is not entirely appropriate for assessing the validity of the different models.

Based on this conclusion, all modelling results were converted to the conversion rate (dX/dt) and then evaluated for the quality of fit. Three statistical parameters were calculated and analyzed: coefficient of determination (R^2), maximum absolute value of relative errors (ME), and average absolute value of relative errors (AE). The parameter values are available in Online Resource 6 (ESM_6), while R^2 and AE are graphically presented in Fig. 4. It should be noted that the isoconversional kinetic models were evaluated only in data range # 1–5, which is the same range they were trained on, and even within this range, they failed to yield sensible activation energies.

Figure 4a, b shows that only the multiple Gaussians model, the FR isoconversional kinetic model (for data # 1–3), and the integrated kinetics-transport pyrolysis model yield positive coefficients of determination, all above 0.90 in these cases. In contrast, the OFW and KAS isoconversional kinetic models failed to describe any data in the dataset, as their R^2 values were always below zero. Comparing the AE values among the models (Fig. 4c, d), these results are consistent with the coefficients of determination. The FR isoconversional kinetic model demonstrates the highest accuracy ($R^2 \geq 0.9934$, $AE \leq 0.110$) in the narrow range (data # 1–3), even though it was trained on a broader dataset (data # 1–5). On the other hand, the multiple Gaussians model and the integrated kinetics-transport pyrolysis model are robust and reliably fit all experimental conversion rate data in this study. The multiple Gaussians model performed the best in this regard with $R^2 \geq 0.9931$, and $AE \leq 0.513$, while the integrated kinetics-transport pyrolysis model performed slightly worse, with $R^2 \geq 0.9117$, and $AE \leq 0.889$.

Correlations between Gaussian parameters and kinetic parameters of the integrated model

To examine potential correlations between parameters obtained by fitting Gaussians and those calculated using the integrated kinetics-transport pyrolysis model, the average values of the Gaussian parameters (a_i, b_i, and c_i) for each individual pseudo-component (i) were calculated and are available in Online Resource 3 (ESM_3). Next, the values of Pearson's correlation coefficient between the Gaussian parameters (a, b, c) and the kinetic parameters of the integrated model (A, E_a, w) were determined. Pearson's correlation measures the strength of the linear association between two variables [32]. Table 5 shows that the pre-exponential factors A have the strongest correlation with parameter c of the Gaussians. Activation energies E_a of the integrated model correlate best with parameter b of the Gaussians. Mass fractions w correlate best with parameter b of the Gaussians. However, no correlation was found between the Gaussian parameter a and any of the parameters of the integrated model.

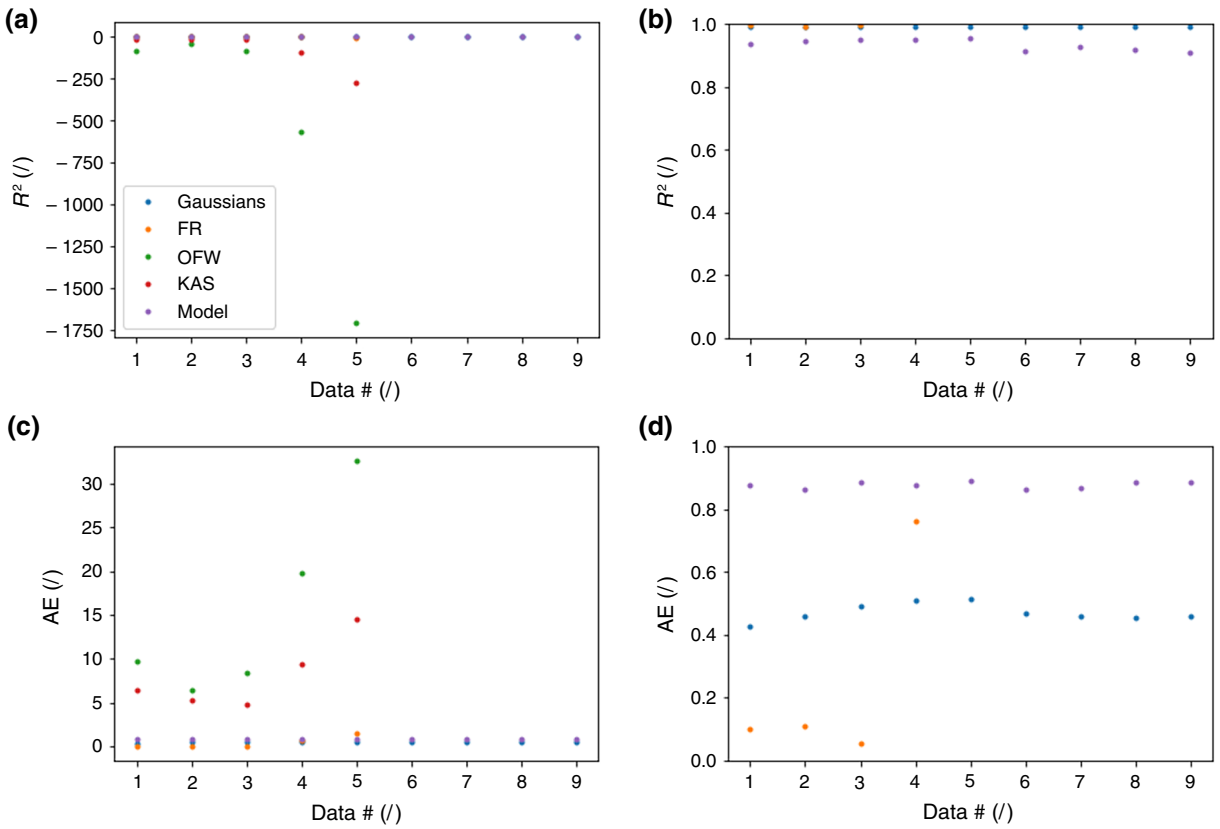

Fig. 4 Direct comparison of the quality of model fits based on conversion rate values is shown using the (R^2) coefficient of determination (**a**, **b**) and the (*AE*) average of the absolute value of relative errors (**c**, **d**). Model refers to the integrated kinetics-transport pyrolysis model

Table 5 Pearson's correlation coefficient between the Gaussian parameters and the kinetic parameters

	a	*b*	*c*
A	−0.5846	0.4572	0.9868
E_a	−0.0307	0.8567	0.7635
w	0.0068	0.8400	0.8278

The Gaussian parameters *b* and *c* can be used to roughly estimate the values of *A* (from *c*), E_a (from *b*), and *w* (from *b*) for individual pseudo-components in spruce wood biomass pyrolysis TG data.

Conclusions

After conducting a case study on spruce wood powder pyrolysis in nitrogen atmosphere to examine several approaches to kinetic modelling of biomass pyrolysis, the following conclusions important to researches involved in biomass pyrolysis modelling can be drawn.

The model with multiple Gaussians is fast, easy to implement, and identifies the main pseudo-components, which is valuable in the initial stages of TG data analysis. The quality of the fits to the actual data is high, with an average coefficient of determination of 0.9933, ranging from 0.9931 to 0.9935. However, the obtained Gaussian parameters do not provide much information about the pyrolysis process on their own. When the correlation between the Gaussian parameters and the kinetic parameters of the integrated kinetics-transport pyrolysis model was assessed, it was observed that the Gaussian parameters could be used to estimate the values of kinetic parameters and mass fractions of individual pseudo-components in spruce wood biomass pyrolysis TG data.

Testing the three isoconversional kinetic models by Fridman (FR), Ozawa-Flynn-Wall (OFW), and Kissinger–Akahira–Sunose (KAS) identified problems with their application to biomass pyrolysis, as already observed and described in the literature [13, 14]. It was found that they display a limited range of applicability (conversion values below 0.825) with adequate coefficients of determination and activation energy values. Statistical evaluation showed that the Fridman (FR) model describes the data well but only at lower heating rates (data # 1–3), while the other two isoconversional kinetic models (OFW and KAS) failed to describe the measured data. Even some good fits of the Fridman (FR) model still had negative activation energy values at

high conversion rates, indicating that the good fits are due to chance rather than accurate description of kinetic behavior under those conditions. Therefore, researchers are discouraged from relying on the results of the tested isoconversional models when applied to biomass pyrolysis data.

The developed integrated kinetics-transport pyrolysis model exhibited relatively high quality of fits for conversion degree, with an average coefficient of determination of 0.9950, ranging from 0.9930 to 0.9964. However, statistical evaluation based on conversion rate values revealed that while the model is robust, its fit quality is slightly lower (average coefficient of determination of 0.9348, with values from 0.9117 to 0.9552) compared to the multiple Gaussians model. The model is highly applicable to pyrolysis of various materials (if the number of pseudo-components and/or reaction order/s are changed) under different conditions (heating rates and carrier gas flow rates), as it models the kinetics of pyrolysis reactions, heat transfer between the temperature sensor and the sample (accounting for potential systematic error in temperature sensing), and external mass transport from the sample to the surrounding fluid. Therefore, the developed integrated kinetics-transport pyrolysis model provides sufficient fit quality across a wide range of experimental conditions, indicating its robustness and versatility, which result from modelling both physical and chemical phenomena during the pyrolysis process.

Supplementary Information The online version contains supplementary material available at https://doi.org/10.1007/s10973-026-15476-6.

Acknowledgements J.V. thanks Mr. Janez Voglar for help in preparing the spruce wood powder sample and Mr. Simon Starašinič for conducting the thermogravimetric measurements. B.L. acknowledges support from the Slovenian Research and Innovation Agency through core funding P2-0152 and project funding J7-4638 and N2-0291. B.L. also thanks the HyBReED program, which is co-financed by the Republic of Slovenia, the Ministry of Higher Education, Science and Innovation, and the European Union–NextGenerationEU.

Author contributions Conceptualization: [Jure Voglar, Blaž Likozar]; Data curation: [Jure Voglar]; Formal analysis: [Jure Voglar]; Funding acquisition: [Blaž Likozar]; Investigation: [Jure Voglar]; Methodology: [Jure Voglar]; Supervision: [Blaž Likozar]; Validation: [Jure Voglar, Blaž Likozar]; Visualization: [Jure Voglar]; Writing – original draft: [Jure Voglar]; Writing – review & editing: [Jure Voglar, Blaž Likozar].

Funding This work was supported by the Slovenian Research and Innovation Agency through core funding P2-0152, project funding J7-4638 and N2-0291, and by the Republic of Slovenia and the European Union through the HyBReED program.

Declarations

Conflict of interest The authors have no relevant financial or non-financial interests to disclose.

References

1. Vikram S, Rosha P, Kumar S. Recent modeling approaches to biomass pyrolysis: a review. Energy Fuels. 2021;35:7406–33.
2. Varghese RT, Antony T, Chirayil CJ. Biomass: abundance, classification, energy potential. Handbook of advanced biomass materials for environmental remediation. Berlin: Springer; 2024. p. 1–12.
3. Sharma A, Pareek V, Zhang D. Biomass pyrolysis—A review of modelling, process parameters and catalytic studies. Renew Sustain Energy Rev. 2015;50:1081–96.
4. Wang Y, Yang S, Bao G, Wang H. Investigation of tobacco straw pyrolysis: three-parallel Gaussian reaction modeling, products analysis and ANN application. Ind Crops Prod. 2023;200:116864.
5. Wang Y, Yang S, Bao G, Wang H. Pyrolysis of macadamia nut peel using multicomponent Gaussian kinetic modeling and ANN analysis. Biomass Bioenergy. 2024;183:107170.
6. Sobek S, Werle S. Isoconversional determination of the apparent reaction models governing pyrolysis of wood, straw and sewage sludge, with an approach to rate modelling. Renew Energy Elsevier. 2020;161:972–87.
7. Cai J, Xu D, Dong Z, Yu X, Yang Y, Banks SW, et al. Processing thermogravimetric analysis data for isoconversional kinetic analysis of lignocellulosic biomass pyrolysis: case study of corn stalk. Renew Sustain Energy Rev. 2018;82:2705–15.
8. Silva JE, Calixto GQ, de Almeida CC, Melo DMA, Melo MAF, Freitas JCO, et al. Energy potential and thermogravimetric study of pyrolysis kinetics of biomass wastes. J Therm Anal Calorim. 2019;137:1635–43.
9. Agnihotri N, Mondal MK. Thermal analysis, kinetic behavior, reaction modeling, and comprehensive pyrolysis index of soybean stalk pyrolysis. Biomass Convers Biorefin. 2024;14:14977–92.
10. Yuan X, He T, Cao H, Yuan Q. Cattle manure pyrolysis process: Kinetic and thermodynamic analysis with isoconversional methods. Renew Energy. 2017;107:489–96.
11. Abdelouahed L, Leveneur S, Vernieres-Hassimi L, Balland L, Taouk B. Comparative investigation for the determination of kinetic parameters for biomass pyrolysis by thermogravimetric analysis. J Therm Anal Calorim. 2017;129:1201–13.
12. Baroni EG, Tannous K, Rueda-Ordonez YJ, Tinoco-Navarro LK. The applicability of isoconversional models in estimating the kinetic parameters of biomass pyrolysis. J Therm Anal Calorim. 2016;123:909–17.
13. Ceylan S, Topçu Y. Pyrolysis kinetics of hazelnut husk using thermogravimetric analysis. Bioresour Technol. 2014;156:182–8.
14. Vyazovkin S, Burnham AK, Criado JM, Pérez-Maqueda LA, Popescu C, Sbirrazzuoli N. ICTAC Kinetics Committee recommendations for performing kinetic computations on thermal analysis data. Thermochim Acta. 2011;520:1–19.
15. Voglar J, Prašnikar A, Moser K, Carlon E, Schwabl M, Likozar B. Pyrolysis of industrial hemp biomass from contaminated soil phytoremediation: kinetics, modelling transport phenomena and biochar-based metal reduction. Thermochim Acta. 2024;742:179899.

16. Babu BV, Chaurasia AS. Pyrolysis of biomass: improved models for simultaneous kinetics and transport of heat, mass and momentum. Energy Convers Manag. 2004;45:1297–327.
17. Kwiatkowski K, Górecki B, Korotko J, Gryglas W, Dudyński M, Bajer K. Numerical modeling of biomass pyrolysis—heat and mass transport models. Numeri Heat Transf A Appl. 2013;64:216–34.
18. Khiari B, Kordoghli S, Mihoubi D, Zagrouba F, Tazerout M. Modeling kinetics and transport phenomena during multistage tire wastes pyrolysis using Comsol®. Waste Manage. 2018;78:337–45.
19. Cano-Pleite E, Rubio-Rubio M, Riedel U, Soria-Verdugo A. Evaluation of the number of first-order reactions required to accurately model biomass pyrolysis. Chem Eng J. 2021;408:127291.
20. Jiang G, Nowakowski DJ, Bridgwater AV. A systematic study of the kinetics of lignin pyrolysis. Thermochim Acta. 2010;498:61–6.
21. Wang C, Shi X, Duan A, Lan X, Gao J, Xiong Q. Kinetic study of the effect of thermal hysteresis on pyrolysis of vacuum residue. Front Chem Sci Eng. 2024;18:145.
22. Jiang Y, Zong P, Ming X, Wei H, Zhang X, Bao Y, et al. High-temperature fast pyrolysis of coal: An applied basic research using thermal gravimetric analyzer and the downer reactor. Energy. 2021;223:119977.
23. Lah B, Klinar D, Likozar B. Pyrolysis of natural, butadiene, styrene–butadiene rubber and tyre components: modelling kinetics and transport phenomena at different heating rates and formulations. Chem Eng Sci. 2013;87:1–13.
24. Alves JLF, da Silva JCG, Languer MP, Batistella L, Di Domenico M, da Silva Filho VF, et al. Assessing the bioenergy potential of high-ash anaerobic sewage sludge using pyrolysis kinetics and thermodynamics to design a sustainable integrated biorefinery. Biomass Convers Biorefin. 2020;1–12.
25. Yasmin T, Asghar A, Ahmad MS, Mehmood MA, Nawaz M. Biorefinery potential of Typha domingensis biomass to produce bioenergy and biochemicals assessed through pyrolysis, thermogravimetry, and TG-FTIR-GCMS-based study. Biomass Convers Biorefin. 2021;1–13.
26. Tarasov D, Leitch M, Fatehi P. Lignin–carbohydrate complexes: properties, applications, analyses, and methods of extraction: a review. Biotechnol Biofuels. 2018;11:1–28.
27. Yeo JY, Chin BLF, Tan JK, Loh YS. Comparative studies on the pyrolysis of cellulose, hemicellulose, and lignin based on combined kinetics. J Energy Inst. 2019;92:27–37.
28. Hajaligol MR, Howard JB, Longwell JP, Peters WA. Product compositions and kinetics for rapid pyrolysis of cellulose. Ind Eng Chem Process Des Dev. 1982;21:457–65.
29. Mani T, Murugan P, Mahinpey N. Determination of distributed activation energy model kinetic parameters using simulated annealing optimization method for nonisothermal pyrolysis of lignin. Ind Eng Chem Res. 2009;48:1464–7.
30. Huang YF, Kuan WH, Chiueh PT, Lo SL. A sequential method to analyze the kinetics of biomass pyrolysis. Bioresour Technol. 2011;102:9241–6.
31. Mishra RK, Mohanty K. Pyrolysis kinetics and thermal behavior of waste sawdust biomass using thermogravimetric analysis. Bioresour Technol. 2018;251:63–74.
32. Sedgwick P. Pearson's correlation coefficient. BMJ. 2012;345.